DOE/CS 40257-1

MASTER

HAGUE INTERNATIONAL
3 ADAMS STREET
SOUTH PORTLAND, MAINE 04106

207/799-1580 207/799-7347

DISCLAIMER

HIGH TEMPERATURE RECUPERATOR TESTS

FINAL REPORT

MAY 1980

Contract No. DE-AC02-79CS40257

Hague International
South Portland, Maine 04106

Prepared by
J. W. Bjerklie
and
R. A. Penty

Hague International Project G-1035
for
The U.S. Department of Energy

Acknowledgements

The authors wish to acknowledge the valuable contributions of Hague International technical personnel and management. Special thanks are due to Paul G. LaHaye, President of Hague International, for his constant support and advice; Christopher Green for installing the system, running the tests, and gathering the data; and Stephen B. Young for his editorial efforts. The support of the Department of Energy for test and demonstration programs is acknowledged, and especially appreciated are the support and suggestions of Dr. John Eustis and Mr. Paul Musser of the Division of Industrial Conservation.

CONTENTS

LIST OF FIGURES

LIST OF TABLES

ABSTRACT

A demonstration and test program was conducted on a high temperature, two pass ceramic tube recuperator. Data pertaining to heat exchanger performance characteristics were collected and compared with calculated values. The effect of improved heat exchanger effectiveness on system fuel consumption was demonstrated. Changes in fuel flow as a function of combustion air preheat while maintaining a given heat load were demonstrated. The effects of excess air on fuel consumption with and without system recuperation were demonstrated.

A preheat level of 1740°F with a heat exchanger inlet of 2537°F for a recuperator effectiveness of 68% was demonstrated. Comparison of test measurements and calculated heat balance and heat transfer characteristics indicated that the measured effects of recuperation and excess air levels on fuel consumption were close to theoretical values.

A post-program examination of the recuperator indicated that no damage to the recuperator occurred that could not be alleviated by minor design modification.

The modifications necessary to achieve 1800 to 2000°F preheat with a ceramic tube recuperator of the type demonstrated were extrapolated from measurements made in this program. The same two pass approach demonstrated in this program can be used. The number of face tubes vs. pressure drop for increased recuperator effectiveness was calculated. Modifications and procedures necessary to achieve a 1800-2000°F preheat with furnace temperatures between 2500°F and 2800°F are discussed.

FINAL REPORT
CONTRACT DE-AC02-79CS40257

HIGH TEMPERATURE RECUPERATOR TEST

1.0 Introduction

1.1 Definition of Goals

Hague International was contracted by the United States Department of Energy to demonstrate the performance of an improved CERHX® heat exchanger. A single pass cross-flow ceramic tube recuperator was modified to a two pass cross-counter flow configuration. A program was run to verify the ability of the modified heat exchanger to provide 1800°F preheated air when operating on a furnace with a chamber temperature of approximately 2600°F. The results of improved heat exchanger effectiveness on system fuel consumption were demonstrated. Changes in fuel flow as a function of combustion air preheat while maintaining a given heat load were demonstrated. Additionally, the effects of excess air levels on fuel consumption with and without system recuperation were demonstrated.

1.2 Recuperator Modifications

Hague International began marketing a standard line of ceramic tube recuperators for use on industrial furnaces in 1978. Maximum air preheat temperature achieved with such single pass, cross-flow units was approximately 1350°F when operating on furnaces with chamber temperatures of 2600°F.

To achieve 1800°F preheat under similar operating conditions with minimal design modifications, a single-pass recuperator was converted to a a two-pass heat exchanger. The necessary design changes were isolated to the two header assemblies. The test facility on which the two-pass heat exchanger was mounted required ducting modifications to handle air preheated up to 400°F higher than normal.

1.3 High Temperature Heat Exchanger Tests

Test runs were performed using one and two burners operating on #2 or #6 oil or propane. The final series of tests was run with one burner firing #2 fuel oil in order to take advantage of the most accurate available fuel metering equipment. The first test was run to meet the major objective of the program: to achieve 1800^{o}F preheated air. Subsequent test runs demonstrated the change in steady state fuel flow with and without the recuperator and with and without large amounts of excess air.

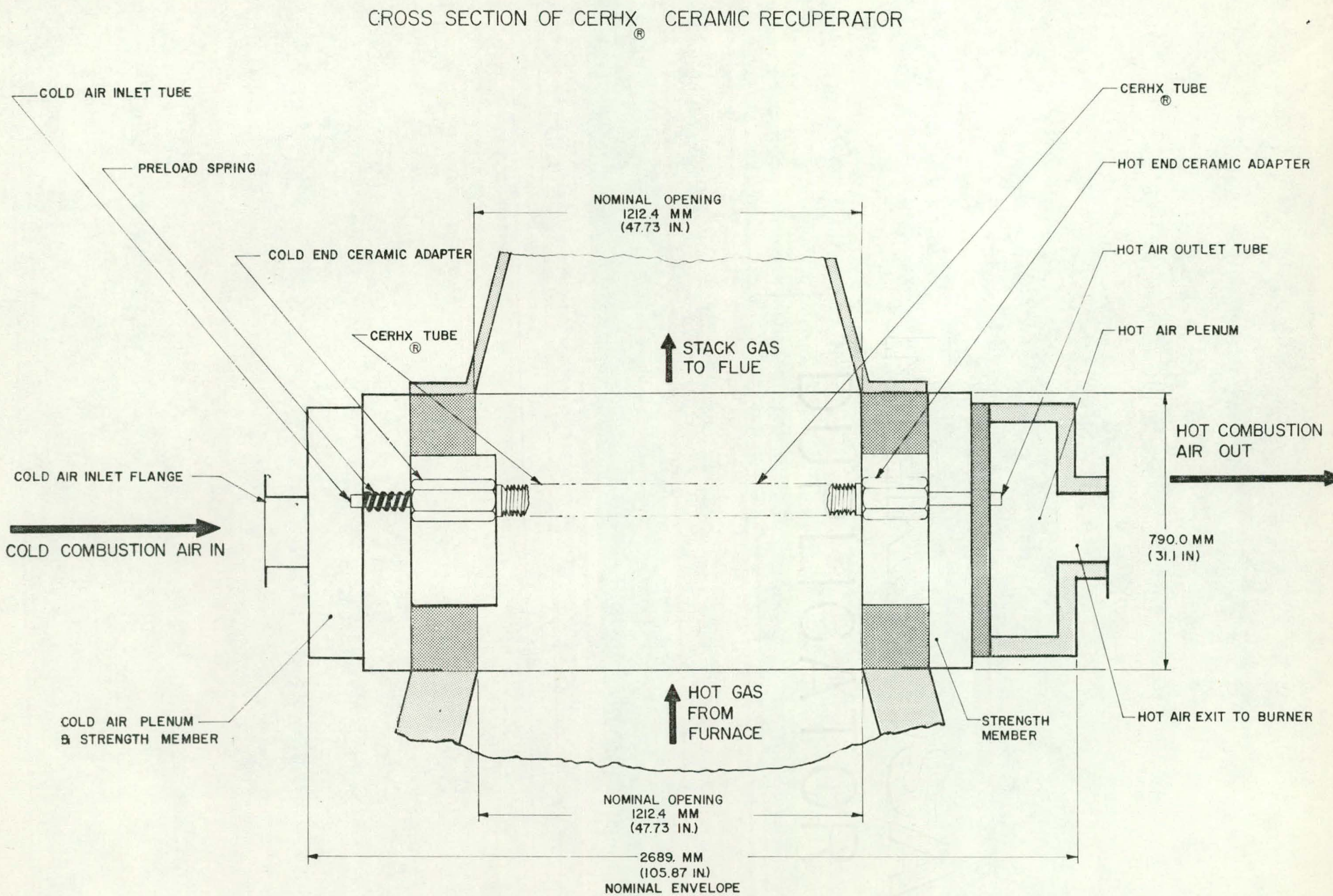

HAGUE INTERNATIONAL
3 ADAMS STREET
SOUTH PORTLAND, MAINE 04106
207/799-1580 207/799-7347

Single Pass Ceramic Heat Exchanger **Figure 1**

2.0 Recuperator Modifications

2.1 The Standard CERHX® Recuperator

A single pass cross-flow Model VI CERHX® recuperator was converted to two pass cross-counter flow recuperator.

Figure 1 is a cross section schematic of a standard single pass cross-flow CERHX® recuperator. The recuperator's structural steel frame is lined with ceramic insulation. The frame, which is closed at its ends, contains the ceramic adapters and the ceramic tubes. A cold air plenum and strongback are located at one end and a hot air plenum and strongback at the other. The individual tubes of the bundle are spring loaded at the cold end, and are held firmly against the hot end strongback.

The tube bundle for the standard recuperator is made up of 30 tubes arrayed in five staggered rows of six tubes each. The bottom row of the recuperator (nearest the furnace) is made up of smooth walled tubes. The other four rows consist of finned tubes.

Each tube string consists of a metal tube extending from the cold header to the cold end ceramic adapter, the ceramic tube, the hot end ceramic adapter, and a high temperature metal tube extending from the hot end ceramic adapter to the hot header. All the tube string components mate with ball and socket joints.

Air flows into the cold header, via a single flange, then spreads and separates to flow in parallel paths through the tube strings. This air is heated in its passage through the tubes and then is dumped into the hot header. The hot air is ducted to the burners via a single flange on the hot header.

2.2 Two Pass Cross-Counter Flow Modifications

Figure 2 is a cross section schematic of the two pass heat exchanger demonstrated in this program.

TWO PASS CERAMIC HEAT EXCHANGER

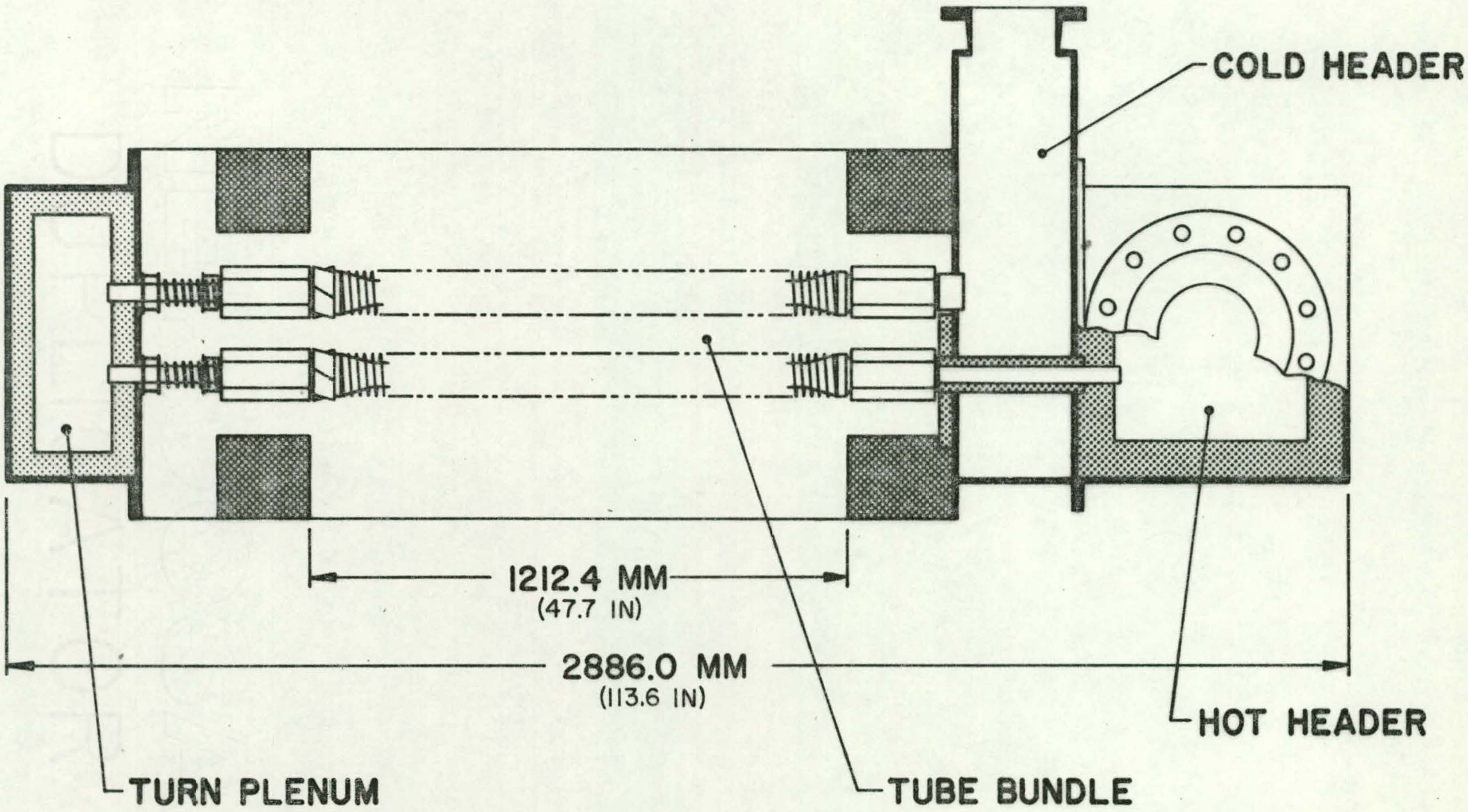

Figure 2

In the two pass heat exchanger, ambient air enters at the rigid end rather than the sprung end. The air is directed into the top two rows of ceramic tubes (i.e., those two rows furthest from the furnace). Flowing through the top two rows, the air becomes partially heated. Partially heated air discharges into what was formerly the cold air header at the sprung end, and turns to enter the bottom three rows of the recuperator (i.e., the three rows nearest the furnace).

The air is further heated when it flows through the bottom three rows of tubes. It finally discharges into a hot header at the rigid end of the recuperator.

This two pass configuration required modification of the standard CERHX® heat exchanger to provide two header plenums at the rigid end of the recuperator. In the one-pass recuperator the rigid end is the location of the hot air plenum, and the sprung end is the location of the cold air plenum. In the two pass recuperator, the rigid end is the location of both the hot air plenum and the cold air plenum. At the sprung end of the two pass recuperator is a "turn plenum" for receiving the partially heated air from the first stage of the heat exchanger, and directing it to the second stage.

The two pass heat exchanger hot header is the outboard box at the rigid end. The cold header is the inboard box at the rigid end.

Cold flow tests were run to determine leakage under deadhead conditions and air side pressure drop under flow conditions. Table 1 shows deadhead leakage. Table 2 shows measured pressure drop in each pass as a function of air flow rate.

3.0 Test Facility

Figure 3 is a schematic of the heat exchanger-furnace test facility used in this program. Figure 4 is a photograph of the test facility.

The recuperator sits on top of the hot gas plenum situated at the rear of the furnace. Process gas flows from the furnace, through both stages of the recuperator to a damper, and then up a stack.

The combustion air delivery system is set up to permit controlled variable bypassing of the recuperators. Air can be directed through the recuperator to the burners, or, with a valve adjustment, can be directed around the heat exchanger directly to the burners. The recuperator can be fully bypassed if desired. Thus the amount of air through the furnace can be set independently of the air flow through the recuperator.

The test facility hot air ducting was rebuilt to give it the ability to accept combustion air heated up to 400°F higher than normal.

Instrumentation for the test runs is shown in Figure 3. Pressure drop and heat exchange data for the first stage of the recuperator (the top two rows) were obtained. The tubes in the bottom row of the recuperator had differing internal diameters and configurations. This created difficulties in measuring flow rates to either the two finned tube rows of the second stage or to the individual tubes in the smooth tube row of the recuperator. Data reduction is feasible for the two finned rows of the second stage of the recuperator if the internal friction factor is assumed to be the same as that measured in the two finned rows of the first stage of the recuperator. This stratagem was used to reduce test data.

The first series of tests was run with two burners. One burner operated on propane, and the other either #6 or #2 fuel oil as desired. The last series of tests was run with a single burner operating on #2 fuel oil.

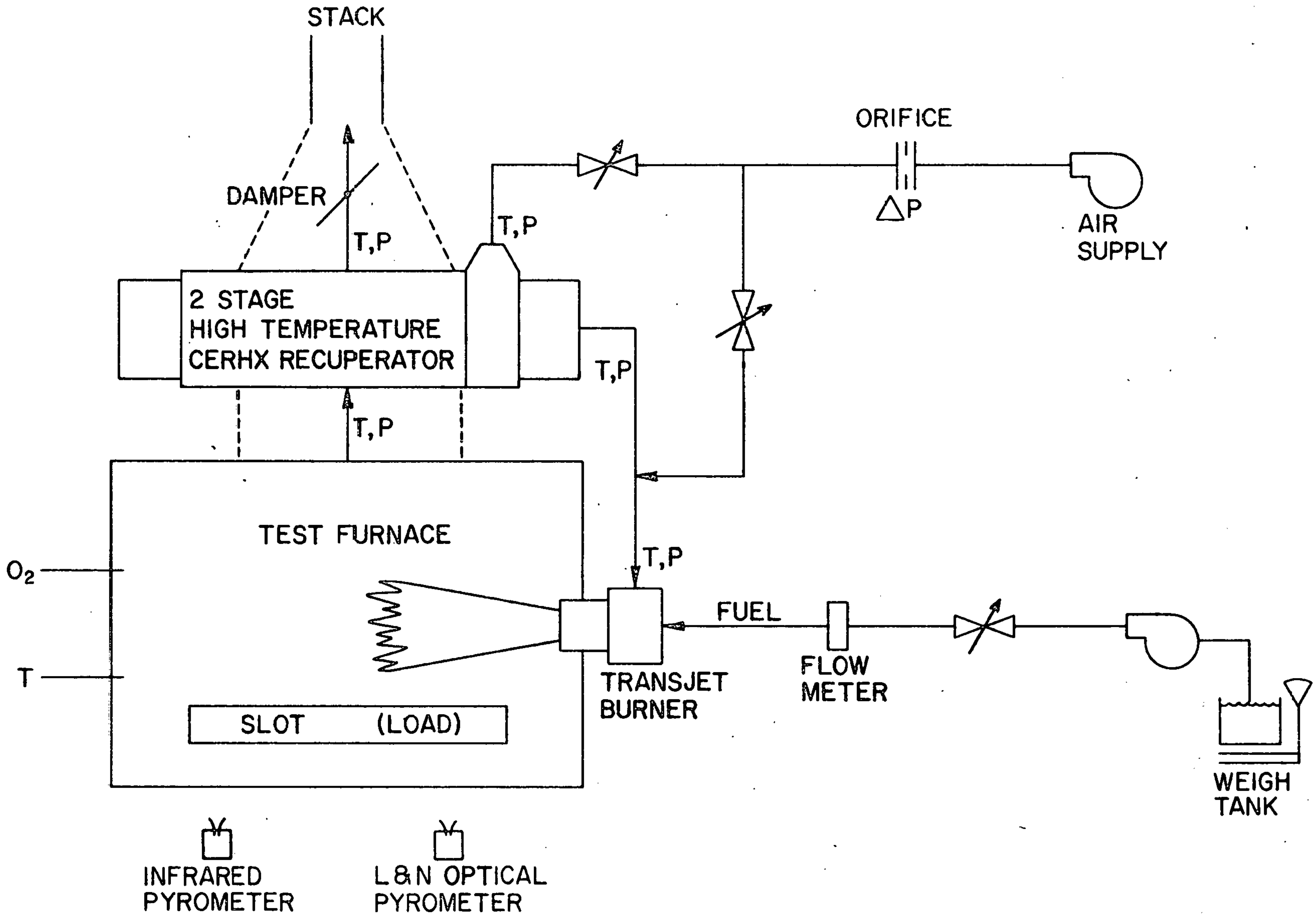

FIGURE 3: TEST FACILITY SCHEMATIC

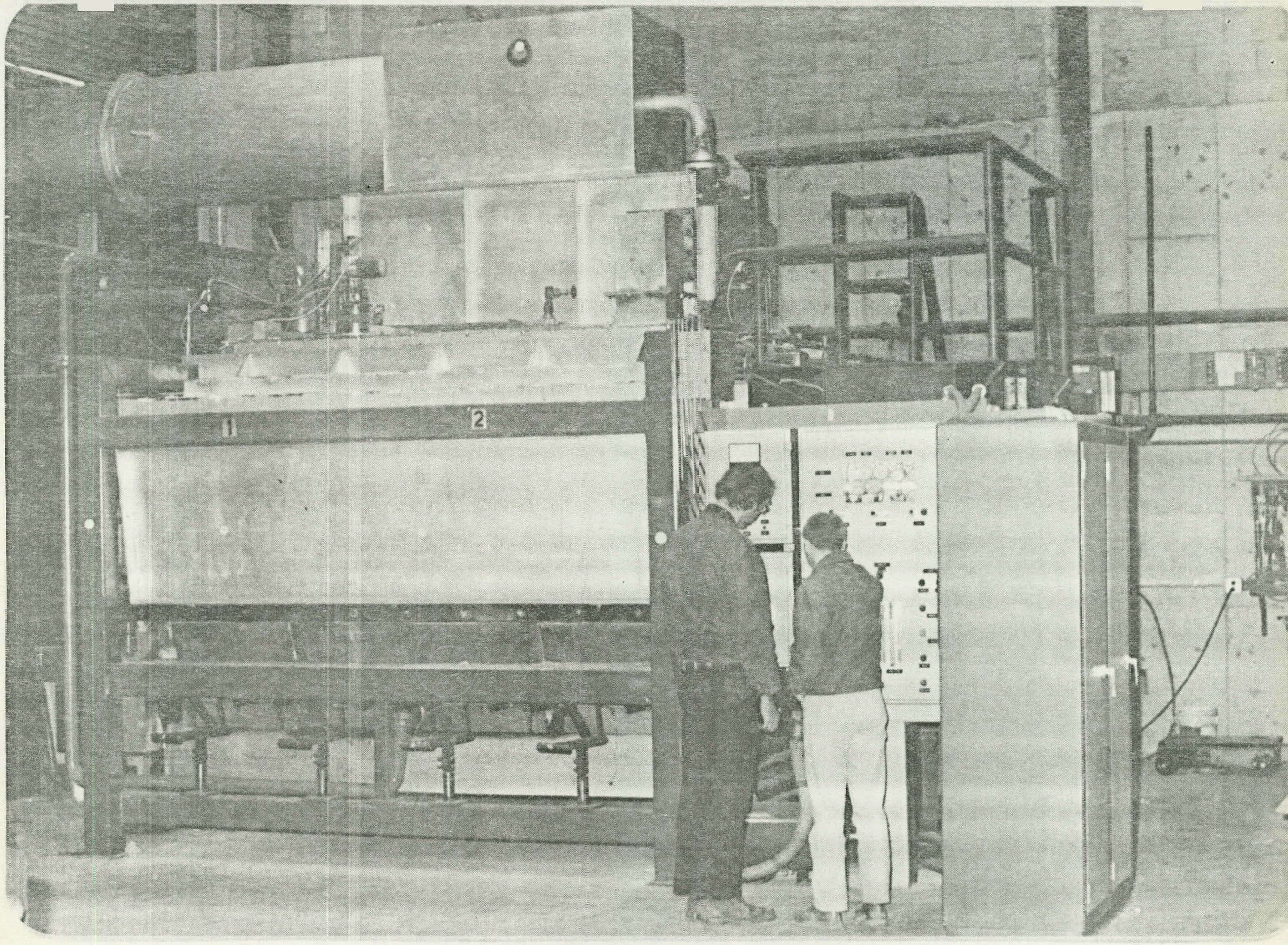

Test Facility **Figure 4**

Fuel flow of #2 fuel oil was measured by a visual rotameter. Flow of #6 fuel oil was measured by a weigh scale and stop watch. Propane flow was calculated by considering the gas burner tip as a calibrated orifice. The methods for measuring #6 oil and propane flow were not as accurate as the method for measuring #2 oil flow. The propane flow measurements made during the final hours of long runs are suspect because of physical changes in the burner tip.

4.0 Theory of Heat Recovery and Recuperation

When air required for a combustion system is preheated by waste heat from that same combustion system, considerable fuel savings can be achieved. Fuel is saved by not having to supply all the heat for the air to get to chamber temperature. Since this means less fuel is needed, there is also less air required for combustion. The relations can be simply presented for a system such as a furnace by forming a heat balance over the furnace envelope. Thus

$$Q_f = \Sigma Q_{loss} + Q_{load} + Q_{stack} + Q_{store} \tag{1}$$

where Q represents heat rates. For a steady state case Q_{store} is zero, the only heat stored being in the load.

The equations hereafter presented assume a pseudo-steady state condition wherein the load heat can be considered independently of the losses. This would be reasonably true for slot forge furnaces, for pusher and rotary furnaces wherein each incremental length of the furnace is at constant temperature, and in batch furnaces after the load is nearly at temperature and is in a hold condition.

Included in the stack losses are air sources and leaks other than the combustion air: e.g. air infiltrated through holes in the structure and hot gas leaked through holes in the structure. After air has been heated, there can be additional air loss through leaks in the ducting structure or recuperator, and additional heat losses from the ducting.

Assuming all heated air leakage occurs after passing through the recuperator, and assuming steady state throughout, including a pseudo-steady state load, we have

$$Q_f = \Sigma\, Q_{loss} + Q_{load} + Q_{\substack{hot\ air\\ leak}} + Q_{\substack{hot\ gas\\ leak}} + Q_{\substack{loss\ hot\\ air\ duct}} + Q_{stack} \tag{2}$$

and $Q_{stack} = (\dot{W}_a + \dot{W}_f + \dot{W}_i - \dot{W}_{gl})\, \bar{C}_p\, (T_s - T_{amb})$

$$Q_{\substack{hot\ gas\\ leak}} = \dot{W}_{gl}\bar{C}_p(T_c - T_{amb})$$

$$Q_{\substack{hot\ air\\ leak}} = \dot{W}_{ahl}\bar{C}_p(T_b - T_{amb})$$

Burner inlet temperature, T_b, can be related to temperature T_{a_o}, and to heat loss in the ducting between the recuperator and the burners. Both T_{a_o} and stack temperature, T_s, can be related to chamber temperature, T_c, by means of the recuperator effectiveness. Thus

$$Q_f = \Sigma Q_{loss} + Q_{load} + \dot{W}_g l_g \overline{C}_p (T_c - T_{amb}) + \dot{W}_a l_a \overline{C}_p (T_b - T_{amb}) \qquad (3)$$
$$+ (\dot{W}_g + \dot{W}_g l_i - \dot{W}_g l_g)\overline{C}_p (T_s - T_{amb})$$

where gas leakage, air leakage and infiltration, are presented as percentages (l_g, l_a, l_i) of ideal combustion gas at any excess air, E. Likewise l_a is the air leakage as a percent of ideal combustion air at any excess air. Ideal combustion gas can be expressed simply as

$$\dot{W}_g = \dot{W}_f\ A/F(1 + E) + \dot{W}_f$$

where A/F is the stoichiometric air-fuel ratio.

Thus

$$Q_f = \Sigma Q_{loss} + Q_{load} + \dot{W}_f \left[(A/F(1+E) + 1\right] \left[l_g C_p \quad (T_c - T_{amb}) + \overline{C}_p \quad (1 + l_i - l_g)(T_s - T_a)\right]$$
$$+ \dot{W}_f\ A/F(1+E) l_a \overline{C}p_{b-a} (T_b - T_{amb}) \qquad (4)$$

or, by relating T_s and T_b to duct losses and recuperator effectiveness, and then dividing through to obtain $\dot{W}_f$:

$$\dot{W}_f \frac{\Sigma Q_{loss} + Q_{load}}{q_f - (T_c - T_a)\left\{ [A/F(1+E)+1] \left\langle l_g \overline{C}p_{c-a} + \overline{C}p_{s-a}(1 + l_i - l_g) \right. \left[1 - \frac{\varepsilon A/F(1+E)(1+l_a)\overline{C}p_{b-a}}{[A/F(1+E)+1]\ (1 - l_i - l_g)\overline{C}p_{c-s}}\right] \right\rangle} $$
$$+ A/F(1+E) l_a \overline{C}p_{b-a} \left[\varepsilon - \frac{Q_{duct}}{W_f A/F(1+E) C p_{b-a}}\right] \Bigg\} \qquad (5)$$

The equation is somewhat simplified if the heat loss from the duct-work is ignored, and also if infiltration, and hot air leakage are considered small or ignored:

$$\dot{W}_f = \frac{\Sigma\ Q_{loss} + Q_{load}}{q_f - \left[A/F(1+E)+1\right]\bar{C}p_{s-a}\left\{\dfrac{\varepsilon A/F(1+E)\bar{C}p_{b-a}}{A/F(1+E)+1\quad Cp_{c-s}}\right\}(T_c - T_a)} \qquad (6)$$

This form of the equation is adequate to show comparison.

The effect on fuel flow of recuperator effectiveness can be determined directly from this equation.

For metallic recuperation systems where the stack gases must be diluted by the ratio, D, of dilution air to stack gas flow in order to reduce the recuperator inlet temperature to a tolerable level, the relation is modified to become:

$$\dot{W}_f = \frac{\Sigma\ Q_{loss} + Q_{load}}{q_f - \left[A/F(1+E)+1\right]\dfrac{\bar{C}p_{s-a}\ \bar{C}p_{c-a}}{\bar{C}p_{i-a}}(T_c - T_a)\left[1 - \dfrac{\varepsilon A/F(1+E)\bar{C}p_{b-a}}{\bar{C}p_{c-i}\left[A/F(1+E)+1\right](1+D)}\right]} \qquad (7)$$

where the subscript, i, refers to recuperator inlet in this case. Figure 5 shows the fuel savings potential for furnaces operating at various temperatures and with recuperators having various effectiveness values.

Equation (6) was used throughout these tests to determine the steady state losses, Q, and to show relative fuel flow with and without the recuperator (ε = .ε or 0 respectively).

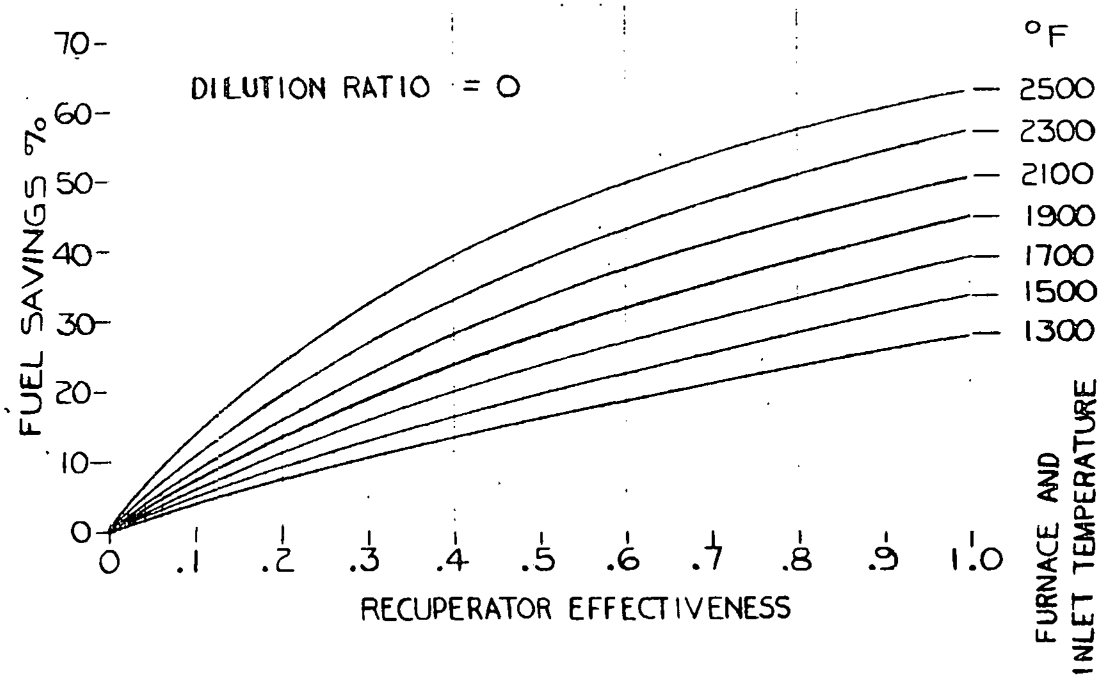

FIGURE 5.

FUEL SAVINGS POTENTIAL AT VARIOUS TEMPERATURE AND RECUPERATOR EFFECTIVENESS VALUES

The effectiveness of a recuperator is a function of its configuration, the flow rates of air and gas, the total heat transfer area, the heat transfer coefficients on air and gas sides, and the thermal conductivity of the heat exchanger material. According to Reference 1, the effectiveness is conveniently represented for each configuration as

$$\varepsilon = f(NTU, \overline{C}_{min}/\overline{C}_{max}) \tag{8}$$

where $NTU - \dfrac{A_s U_s}{\overline{C}_{min}}$, or $\dfrac{A_o U_o}{\overline{C}_{min}}$

when referred to outside tube surface

and $\overline{C}_{min} = \dot{W}_{min}\,\overline{C}_{p_{w_{min}}}$

$C_{max} = \dot{W}_{mas}\overline{C}_{p_{w_{max}}}$

For the usual furnace without air dilution of the stack gases

$$C_{min} - \dot{W}_a \bar{C}_{p_{b-a}}$$

$$C_{max} = \dot{W}_g \bar{C}_{p_{c-s}}$$

Also

A_o = total outside area of the recuperator tube

U_o = overall conductance of the heat exchanger tubes referred to the outside surface

The overall conductance can be expressed as

$$U_o A_o = \frac{1}{\frac{1}{h_o} + \frac{A_o/\bar{A}_w}{(k/t)_w} + \frac{A_o/A_i}{h_i}}$$

where $\bar{A}_w$ = total log mean tube wall area = $\pi d_{lm} L$

L = tube length

d_m = log mean diameter of the tube wall

k_w = thermal conductivity of the wall material

t_w = wall thickness

h_o = external equivalent convective heat transfer coefficient

h_i = internal heat transfer coefficient

A_i = total internal tube area

$= PL = \frac{4A_f L}{d_h}$

A_f = internal flow area of tube

d_h = hydraulic diameter of tube

P = wetted perimeter of the tube cross section

The expression for the conductance can be summed over many tubes or taken as a complete heat exchanger.

Testing tubes for heat transfer coefficients depends on determining the heat transferred and relating it through measured temperature to obtain U and the heat transfer coefficients:

$$Q = W_a C_p \left(\Delta T_{air} \right) = U_o A_o (\overline{T}_g - \overline{T}_a)$$

where T_g and T_a are the mean temperatures of the gas and air at the tube being analyzed.

The known values in the U equation are k/t, A_w, A_o, and A_i. Both h_o and h_i are to be determined.

5.0 Test Results

5.1 High Temperature Test

The furnace was started on two burners, one burning propane and the other burning #6 fuel oil. A firing rate averaging 2.2×10^6 Btu/hr was maintained to heat the furnace chamber temperature to 2500°F, and hold it between 2500-2700°F. The furnace temperature gradually crept upward during the next 16 hours, until it reached 2700°F. Ten air outlet temperatures were monitored at the air exit of the recuperator's second stage: 4 on the bottom row, 2 on the second row, and 2 on the third row. Figure 6 shows these outlet temperatures and the chamber temperature displayed as a function of time.

The air outlet temperatures from the first stage are also shown in Figure 6.

The pressure drops on the gas side of the recuperator and across the air flow orifice were monitored on an "as needed" basis. Gas side pressure drop as a function of total air flow plus fuel flow is shown in Figure 7. Pressure drop on the air side of the recuperator is not shown, as some air was bypassing the recuperator and these figures would be for a derived rate.

The air flow measurement includes the air flow to the burners, any duct leakage, and any recuperator leakage. Cold flow tests were run to evaluate the effectiveness of the seals in the recuperator. The seals reduced leakage to negligible levels.

Deadhead tests were run to determine the flow correction due to leakage of the tube assembly. This leakage is shown in Table 1.

Air flow as measured by the orifice can be considered a true value only during the first part of the high temperature run, as minor additional leakage may develop as the tubes grow and contract with cycling.

Air flow can be checked by knowing the air flow through the burners. All

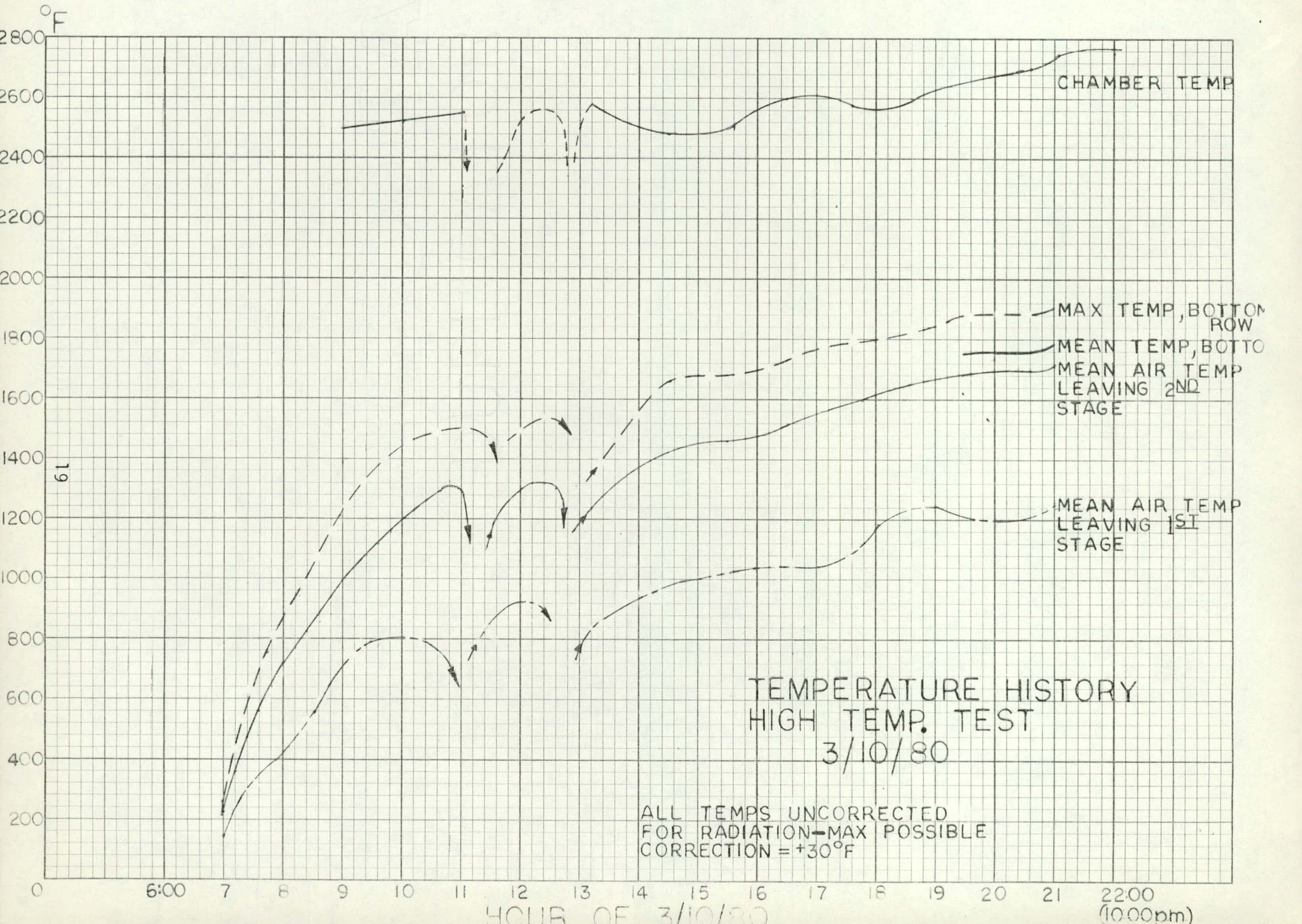
°F
2800
2600
2400
2200
2000
1800
1600
1400
1200
1000
800
600
400
200
0
CHAMBER TEMP
MAX TEMP, BOTTOM ROW
MEAN TEMP, BOTTO
MEAN AIR TEMP LEAVING 2ND STAGE
MEAN AIR TEMP LEAVING 1ST STAGE
TEMPERATURE HISTORY
HIGH TEMP. TEST
3/10/80
ALL TEMPS UNCORRECTED FOR RADIATION—MAX POSSIBLE CORRECTION = +30°F
6:00
7
8
9
10
11
12
13
14
15
16
17
18
19
20
21
22:00 (10:00pm)
HOUR OF 3/10/80

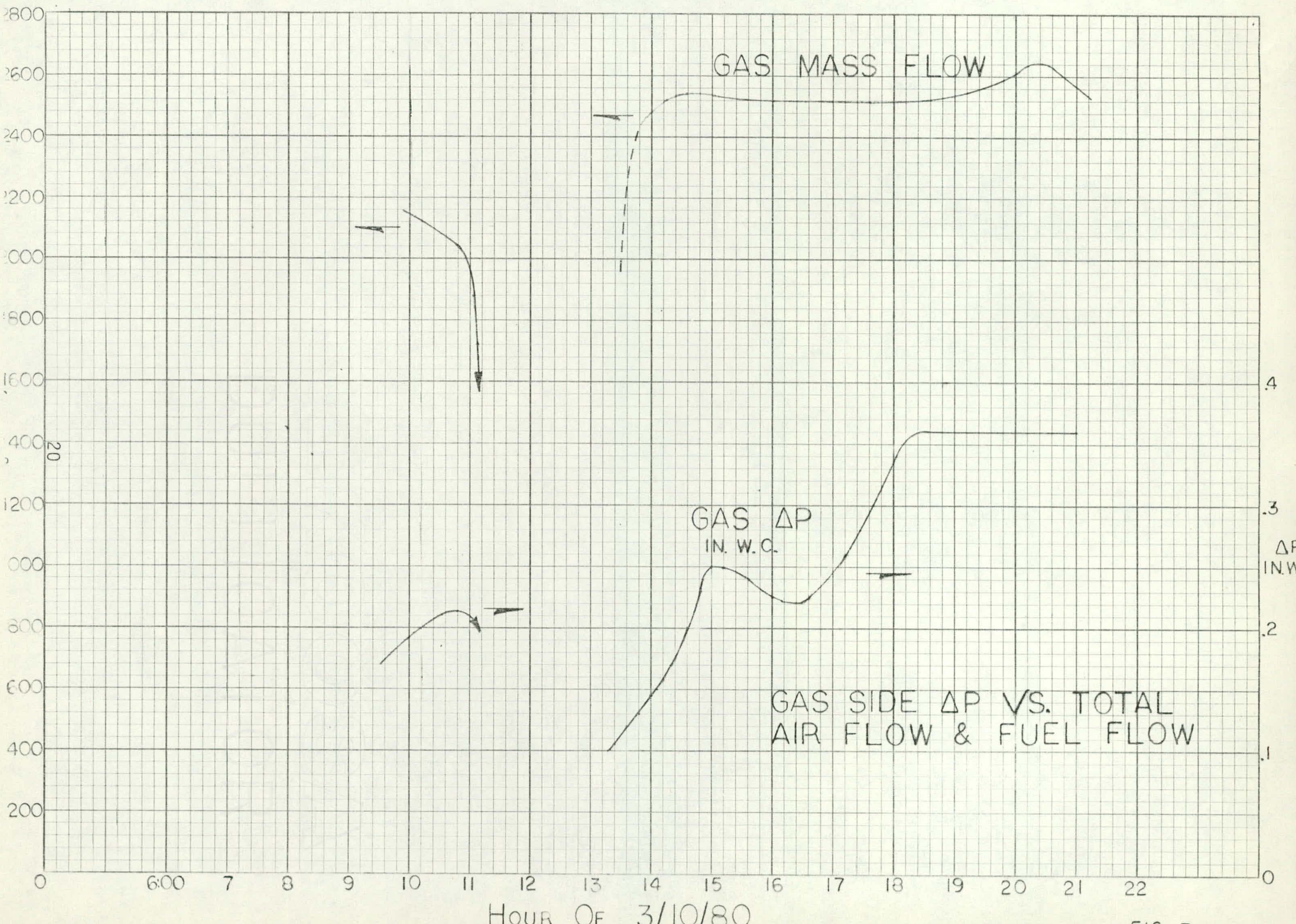
GAS MASS FLOW
GAS ΔP
IN. W.C.
GAS SIDE ΔP VS. TOTAL
AIR FLOW & FUEL FLOW
ΔP
IN.W
0
200
400
600
800
1000
1200
1400
1600
1800
2000
2200
2400
2600
2800
20
.1
.2
.3
.4
6:00
7
8
9
10
11
12
13
14
15
16
17
18
19
20
21
22
Hour Of 3/10/80

FIG. 7

the air from the recuperator must flow through the burners, except for duct leakage, which was essentially zero during the cold flow runs. Tables 2 and 3 show the air flow and pressures measured on the furnace during cold flow. The friction factor for air flow was calculated for the first stage from these measurements.

Since the furnace was closed during the cold flow tests, the pressure drop on the gas side of the recuperator could be measured. The air that flowed through the recuperator dumped into the furnace through the burners, and then flowed through the recuperator. The measured pressure drop was used to calculate the gas side friction factor. These friction factor results were plotted along with the calculated friction factor from hot runs (Figure 8).

Only the flow rates through the top two tube rows (first stage) were sufficiently well defined for evaluating air side friction factor. The second stage consisted of two rows similar to the two rows of the first stage, but had a third row made up of smooth wall tubes of several different internal diameters and configurations. Thus friction and heat transfer evaluations were applied to the finned tubes only.

The maximum temperature run included some bypass of combustion air around the recuperator. Thus the air through the recuperator was only about 68 % of the total air to the burners. This condition was selected during the run so as to show the ability of the heat exchanger to achieve temperatures at, or close to, 1800°F.

The exit temperature from the recuperator was taken as the average of average exit temperatures from the three rows of the second stage. The highest of these averages was 1740°F (with correction) when the recuperator gas inlet temperature was 2537°F. The effectiveness corresponding to these temperatures is 68%.

The chamber temperature at this time was 2750°F. The most reliable data from these tests are the gas side flow rate, the gas side inlet temperature, and the

[redacted]

FIGURE 8

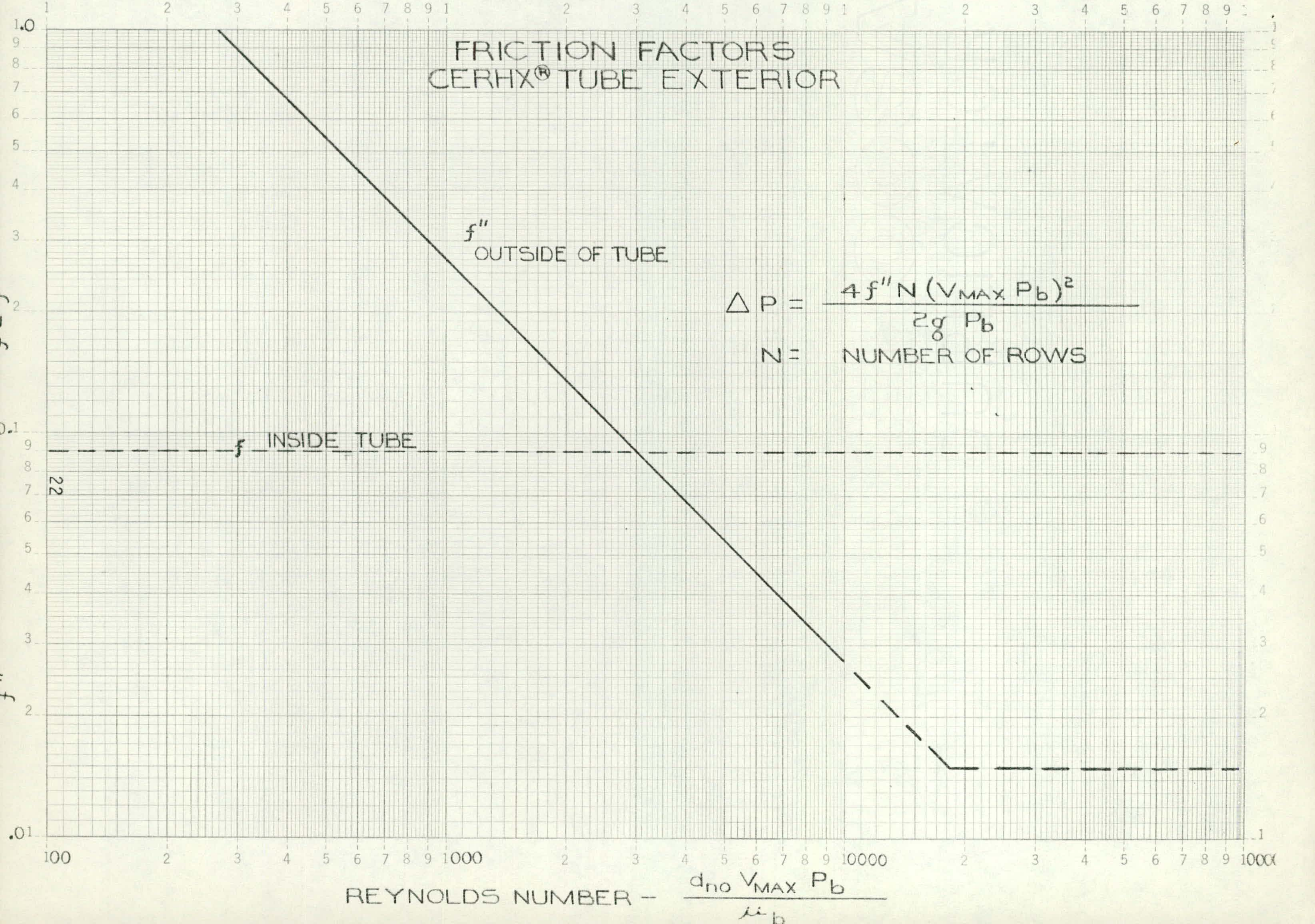

air side temperatures. A heat balance between the flows on the two sides of the recuperator dictates

$$\dot{W}_a \underline{\overline{C}_{pa}}(\underline{T_{ao}} - \underline{T_{ai}}) = \underline{\dot{W}_g}\ \underline{\overline{C}_{pg}}\ (\underline{T_{gi}} - T_{go})$$

The known data terms are underlined. Also, the recuperator effectiveness is a reliable value, therefore

$$\underline{\varepsilon} = \frac{\underline{T_{ao}} - \underline{T_{ai}}}{\underline{T_{gi}} - \underline{T_{ai}}} = \frac{\underline{\dot{W}_g}\ \underline{\overline{C}_{pg}}\ (\underline{T_{gi}} - T_{go})}{\dot{W}_a\ \underline{\overline{C}_{pa}}\ (\underline{T_{gi}} - \underline{T_{ai}})}$$

The known data terms are again, underlined. Since there are two independent equations, we can evaluate W_a and T_{go} fairly reliably. From this the ratio

$$\frac{\dot{W}_g \overline{C}_{pg}}{\dot{W}_a \overline{C}_{pa}} = C\ max/_{C\ min}$$

can be determined.

Values of $C\ max/_{C\ min}$ can be used to enter the ε vs. NTU and $C\ min/_{C\ max}$ curves of Reference 1. The ratio of ε values of $C\ min/_{C\ max}$ as determined here (=.55) to that for $C\ min/_{C\ max}$ for nonleaking, non-bypassing recuperative system (=.75 for gas and air temperature as measured in the tests reported here) is a near constant .95 for a range of ε values near that indicated from the tests. This means that for the demonstration heat exchanger with its measured effectiveness of 68%, the effectiveness would have been 64.5% if used purely as a recuperator.

The preheat that would be expected for the identical heat exchanger used purely as a recuperator on a furnace operating at 2700°F (2550°F gas temperature at the recuperator inlet) would have been 1600°F. This value is lower than originally anticipated.

The anticipated value of effectiveness for the configuration flow rates and gas temperatures tested was 70%

5.2 Recuperative Tests

The second set of tests was run to show the variation of flow rate with preheat. The heat transfer rates in these fully recuperated cases could be evaluated with some reliability.

Table 4 shows the heat rates for various thermal conditions. In particular, comparison is possible between loaded and unloaded when fully recuperated, loaded and unloaded when fully bypassed, and between recuperated and non-recuperated when unloaded. "Load" in these cases represents the difference in combined radiation and convective loss from the closure used to fill the slot of the test furnace between two measurable extremes. That is, when the slot closure was insulated from the outside,the loss could be estimated from the measured external surface temperature. Also, when the insulation was removed another loss could be estimated for the unprotected brick used to close the slot. The difference between these losses was the "load".

It should be pointed out that removal of the slot closure entirely would represent a much larger load, but would not have been practical for running long periods in the test facility because of hazards to personnel and the surrounding equipment. Therefore, the compromise of using insulated or uninsulated slot closures was adopted.

Only the most valid data points could be used to draw the heat rate comparisons for recuperated vs. non-recuperated cases. "Validity" was defined when a heat balance could be formed between fuel heat and total heat loss. This required that a measure of the total heat loss be made. This was conveniently found by extended operation of the furnace in the unloaded state such that temperatures of the walls, stack gas, and preheated air were no longer varying. The most valid data appeared to be those for the unloaded, unrecuperated case:

$$Q_f = \Sigma Q_{loss} + Q_{stack}$$

from point

$$\Sigma Q_{loss} = 740{,}000 \text{ Btu/hr}$$

This value was then applied to other cases to pick those that showed a heat balance within $\pm$15%. These points are indicated with (OK).

Comparative points can be established by forming ratios of heat rate between two conditions taken closely together in time even if the heat balance is not correct. In this case, the heat balances should, at least, be unbalanced in the same direction by the same ratios. The points indicated with (**) were compared in this manner.

Table 5 shows the ratios of heat rates between selected pairs. It was clear that "loading" increased fuel flow over "unloaded", as expected; that "non-recuperated" increased fuel flow over "recuperated", as expected; and that excess air increased fuel flow, as expected. The theoretical ratios of "loaded to unloaded" are shown using the measured load differences. Only the steady state cases can be used for this comparison since an unbalanced heat load represents a bias not necessarily in proportion when comparing two cases. Theoretical ratios of recuperated vs. unrecuperated were calculated using the apparent effectiveness

$$\varepsilon = \frac{(\overline{T}_{ao} - T_{ai})}{T_{gi} - T_{ai}}$$

when fully recuperated. The basic conclusion to be drawn is that the effect of the recuperator on fuel flow is close to theoretical.

The balanced, fully recuperated cases were evaluated to determine the effective overall heat transfer (U) value in the finned tubes of the first and second stage. The general procedure was as follows:

determine an air flow rate by checking air flow measured by the orifice and air flow estimated by the burner flow;

determine fuel flow;

form a heat balance across the recuperator using $\dot{W}_a$, $\dot{W}_g$, T_{gi}, T_{ai}, T_{ao} ------ T_{go} must be equal to or higher than the measured T_{go};

pick the $\dot{W}_a$ that results in a T_{go} considered to be most valid;

using this $\dot{W}_a$, find ΔT_g in first stage, and calculate f 1st stage;

using f_{2nd} stage = f_{1st} stage estimate $\dot{W}_{a2nd}$ stage for the finned tubes;

determine ΔT_g in second stage;

find U_o of all four finned tube rows.

Figure 9 shows the measured overall conductance of the ceramic tubes (U_o) as a function of mass flow in pounds per hour. The cooler first air stage is described by a different curve than the two finned tubes of the second air stage. This is due to the much higher viscosities in the second stage. The bottom row of smooth tubes is described by a third curve because of its different internal sizes.

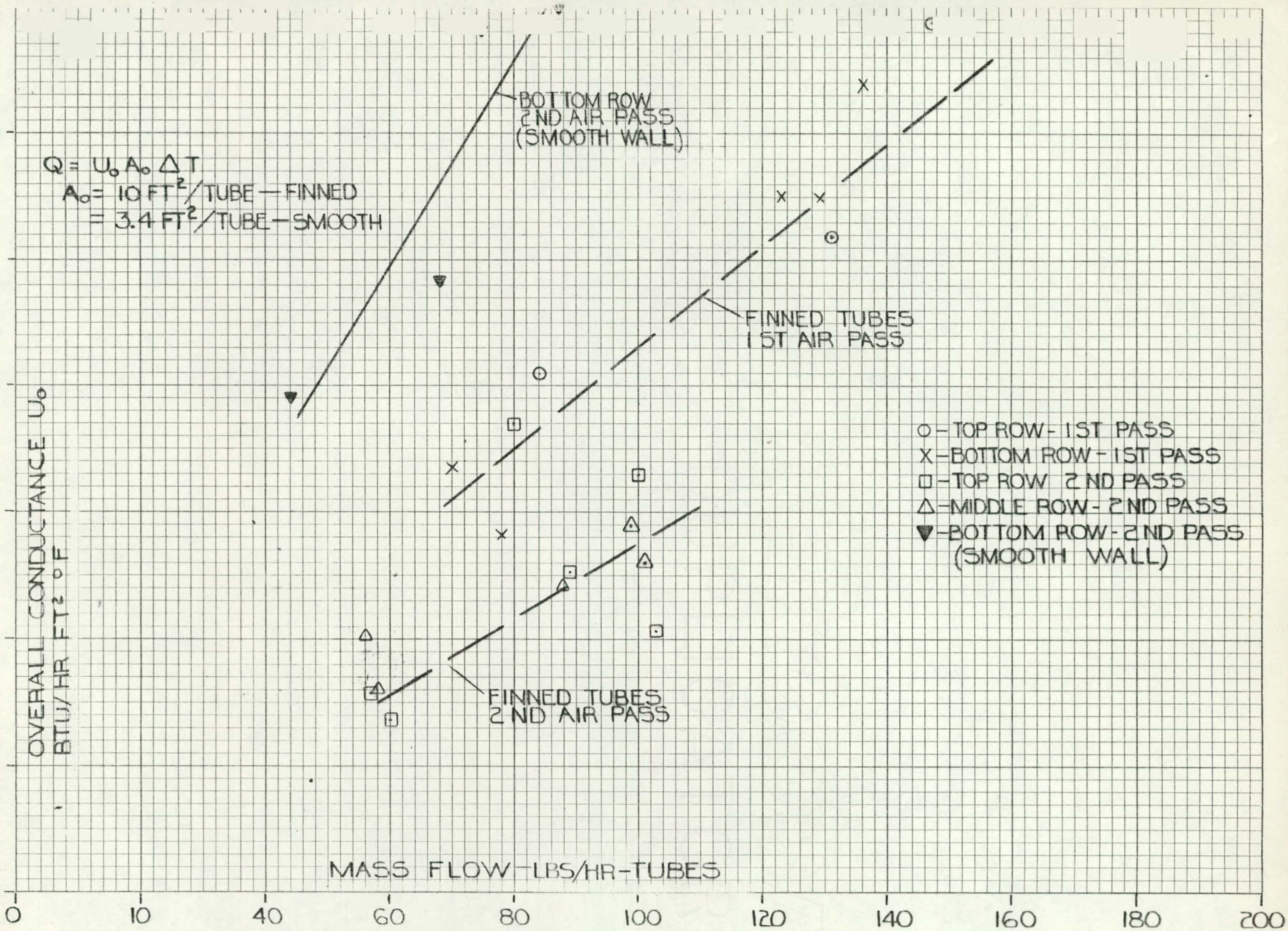

FIGURE 9

MEASURED OVERALL CONDUCTANCE OF CERAMIC TUBES

5.3 Inspection of the Recuperator

The recuperator suffered some damage due to the high air outlet temperatures. One finned tube in the second row of the recuperator (the middle row of the second air pass) was found to be cracked in place. There was no drastic air leakage. Springs became partially relaxed. Minor redesign of the recuperator would alleviate all the conditions that caused the damage.

5.4 Design for 1800°F Recuperator

Using the heat transfer coefficients obtained from test measurements and factoring in the findings of the post-program inspection of the recuperator, it is possible to define the modifications necessary to increase the effectiveness of a ceramic recuperator of the type demonstrated to 72% in order to achieve the goal of 1800°F preheat with 2500°F inlet temperature. Evaulation was made for a fuel input of 2 x 10^6 Btu/hour to the system.

The same two pass approach demonstrated can be used, with the top two rows constituting the heat exchanger's first pass and the three bottom rows constituting the second pass.

With these conditions 7 rather than 6 columns of tubes are required for 72% effectiveness. The first air pass outlet temperature would be 1116°F, and the final air temperature would be 1800°F. The gas side pressure drop would be 0.14 inches w.c. The original concept for a high temperature heat exchanger was satisfactory except that the recuperator needs to be increased in size.

An 80% effective recuperator can be achieved by either increasing recuperator size (adding columns of tubes) or by going to a three pass arrangement. A three pass arrangement would require extensive but not particularly difficult changes to the recuperator design.

6.0 Conclusions and Recommendations

The recuperator, when operated as a heat exchanger with less air than required for combustion, demonstrated a corrected mean exit temperature of 1740°F. This corresponds to an effectiveness of 68%. Extrapolating the data to fully recuperative conditions, i.e. with air flow through the heat exchanger tubes sufficient to generate the total gas flow around the tubes, shows that a probable effectiveness of 64.5% would have been achieved in fully recuperative conditions. A recuperator similar to the one demonstrated with one more column of tubes would have achieved 1800°F preheat under test conditions.

The recuperator suffered some damage due to the high air outlet temperatures. Springs became partially relaxed, and one tube in the middle row of the second air pass broke. Minor redesign would alleviate all the conditions that caused this damage.

To achieve 1800°F to 2000°F preheat with furnace temperature in the range of 2500-2800°F, the following recommendations are made:

(1) Conduct tests to clarify the air side heat transfer and pressure drop coefficients at high air temperatures.

(2) Conduct tests to verify the gas side heat transfer and pressure drop coefficients.

(3) When reliable heat transfer and pressure drop coefficients are available, resize and rebuild the recuperator to accept flow from two burners. Equip the furnace with a sizable thermal load to assure the availability of gas and air flow rates typical of systems of the same physical size operating in the field. Perform a demonstration program to confirm improved recuperator performance.

TABLE 1

Dead Head Leakage - 2 Pass Heat Exchanger

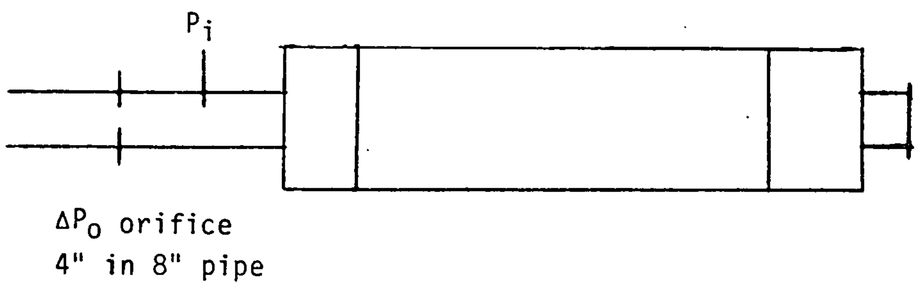

P_i	ΔP_{orif}	$\dot{W}_a$
29 in. w.c.	.05 in. w.c.	220 lbs./hour

TABLE 2

Cold Flow Tests: ΔP and $\dot{W}_{air}$

P_i (in. w.c.)	ΔP_o (in. w.c.)	1st air pass* ΔP_1 (in. w.c.)	2nd air pass** ΔP_2 (in. w.c.)	$\dot{W}_a$ (lbs./hr.)
25.6	7.2	13.8	5.7	2600
16.4	4.75	9.1	3.7	2110
7.7	2.3	4.4	1.7	1480

$f = .074$

* 12 - standard CERHX® finned tubes, d_h = .0238

** 12 - standard CERHX finned tubes, d_h = .0238
+ 4 smooth wall tubes, d_h = .027
+ 2 smooth wall tubes, d_h = .16

TABLE 3

Flow Tests with Recuperator on Furnace

P_i (in. w.c. avg. at two burners)	ΔP_o (in. w.c.)	$\dot{W}_a$ (lbs./hr.)	$\Delta P_{gas\ side}$ (in. w.c.)	$T_{i_{gas\ side}}$ (^oF)	N_{Re}
8.3	21	4450	0.35	1040^oF	775 (based on d_h = .0222').

TA[illegible] 4

FURNACE HEAT RATES

	Run Date	Run Time	$\dot{W}_f$ (lbs./hr.)	Recup-erated	Load (Btu/hr.)	Measured heat in fuel Q_f (Btu/ hr.)	O_2	Tb (^oF)	Theoretical heat in Fuel Q_f (a) (Btu/hr.)	Accept-ability of heat balance (c)	Acceptability of paired test points for compariso
1	3/18/80	11:00	118(#6)/70P	No	118,200	4.5×10^6	1.5%	290	2.09×10^6		Marg
2		12:10	12(#6)/92P	No	0	2.105	1.5	260	2.18	O.K.	
3		13:00	24(#6)/108P	No	0	2.65	7.0	187	3.37		O.K.
4		14:00	60(#6)/107P	No	149,000	3.282	6.0	182	3.69	O.K.	O.K.
5		15:17	12(#6)/100P	Partial	163,000	2.268	1.5	1090 (1714)(b)	2.01	O.K.	
6		16:18	12(#6)/52.5P	Partial	0	1.294	1.5	1359 (1660)	1.64	Marg	
7		17:30	12(36)/37P	Partial	0	.976	10.0	941 (1643)	1.81		
8		18:35	6(#6)/37P	Partial	156,000	.867	10.3	1046 (1530)	1.65		
9	3/19/80	11:00	72(#6)/58P	Yes	149,000	2.497	1.0	1093 (1220)	1.595	Marg	
10		12:17	51(#6)/37P	Yes	163,000	1.683	1.0	1144 (1306)	1.289	Marg	
11		13:05	48(#6)/33P	Yes	179,200	1.547	0	1200 (1369)	1.30	O.K.	O.K.
12		17:01	32(#6)37P	Yes	0	1.339	1.0	1200 (1373)	1.005		
13	3/20/80	13:34	65.7(#2)/77P	Yes	0	2.774	4.5	1045 (1143)	1.741		
14		14:53	65(#2)/77P	Yes	100,000	2.76	4.5	1125 (1228)	1.7		
15	4/29/80	12:00	70(#2)	Yes	170,300	1.27	1.6	1228 (1364)	1.26	O.K.	O.K.
16		20:00	61.3(#2)	Yes	0	1.11	1.5	1270 (1420)	1.044	O.K.	
17	4/30/80	1:55	92(#6)	No	181,500	1.67	1.0	182	1.63	O.K.	
18		3:10	83.4(#2)	No	173,500	1.51	1.5	181	1.64	O.K.	O.K.
19		4:30	68(#2)	No	0	1.23	2.2	144	1.42	O.K.	
20		6:00	35(#2)	Yes	0	.635	3.5	1265 (1542)	.99		O.K.

a) Assumes ΣQ_{loss} = 740,000 Btu/hr., and $Q_f = \left[(\Sigma Q_{loss} + Q_{load})/\bar{q}_f - \left(\frac{\dot{W}_a + \dot{W}_f}{\dot{W}_f}\right)\bar{C}_p(T_{go} - T_a)\right] \times \bar{q}_f$ and using T_{go} derived from recuperator heat balance on all recuperator runs.

b) Temperatures in parentheses are recuperator air outlet values.

c) Acceptability OK if Q_f theoretical/Q_f measured = $1 \pm .2$

TABLE 5

HEAT RATES OF SELECTED PAIRS

Data Point From Table 4	Date of Run	Clock Time Of Run	Recup	Load (Btu/hr.)	T_{ao} (°F)	T_{gi} (°F)	Fuel Heat Rates: Effect Of Increased Load	Fuel Heat Rates: Effect Of Using Recup-eration	Fuel Heat Rates: Effect Of Increased Excess Air
2.		12:10	No	0					1.26 *
3.		13:00	No	0			1.24		1.53
4.		14:00	No	149,000			1.1		
11.	3/19/80	13:05	Yes	179,200	1369	2170	1.16		
12.		17:01	Yes	0	1373	2180	1.24		
15.	4/29/80	12:00	Yes	170,300	1364	2120	1.14		
16.		20:00	Yes	0	1420	2222	1.21		
18.	4/30/80	3:10	No	173,500			1.23		
19.		4:30	No	0			1.22	.516	
20		6:00	Yes	0	1542	2288		.69	

*Upper numbers in brackets compare ratio of measured fuel heat between the two runs subtended by the brackets; the lower numbers compare the ratio of theoretical fuel heats. Heat rates shown on Table 4.

7.0 References

1. W.M. Karp and A.L. London, Compact Heat Exchangers, Palo Alto, California, 1955.

2. K.G. Hagen, High Pressure Ceramic Heat Exchanger Phase 1 - Deadhead Experimental Verification, prepared for the United States Department of Energy Industrial Conservation Division, Contract No. EC-77-C-02-4236, Mod A005, 1979.

3. W.M. Rohsenow and J.P. Hartnett, eds., Handbook of Heat Transfer, New York, 1973.

4. W.H. McAdams, Heat Transmission, New York, 1954.